Indian Journal of Chemistry
Vol. 44A, May 2005, pp. 956-967

Kinetic evaluation of the standard rate constant from cyclic voltammetric data at SWCNT-modified tungsten microelectrodes

A Curulli[1,*], F Valentini[2], S Orlanducci[2,3] & M L Terranova[2,3]

[1] Istituto Materiali Nanostrutturati (ISMN) CNR Division 2, via del Castro Laurenziano 7, 00161 Rome, Italy
[2]Dipartimento di Scienze e Tecnologie Chimiche Università degli Studi di Roma Tor Vergata, via della Ricerca Scientifica 1, 00133 Rome, Italy
[3] INSTM (Consorzio Nazionale Scienze e Tecnologie dei Materiali) Università degli Studi di Roma Tor Vergata, via della Ricerca Scientifica 1, 00133 Rome, Italy
Email: antonella.curulli@uniroma1.it

Received 9 November 2004

The electrochemical properties and the kinetic evaluation at Single-Walled Carbon Nanotubes (SWCNTs) -modified tungsten (W) microelectrodes have been studied and compared with those of Glassy Carbon (GC) bare electrodes. Field Emission Scanning Electron Microscopy (FEG-SEM) and Raman spectroscopy have been used to characterize the modified-electrode morphology and microstructure, respectively. Cyclic voltammetry (CV) has been used to study the electrochemical performances, with seven different redox systems serving as probes ($Fe(CN)_6^{3-/4-}$; $Ru(NH_3)_6^{3+/2+}$, $Ir(Cl)_6^{2-/3-}$, catechol, dopamine, ferrocene monocarboxylic acid and caffeic acid). The analytical response for different systems is highly reproducible for each type of tungsten microelectrode modified with SWCNT coating by Chemical Vapor Deposition method (CVD). For all seven redox systems, the forward reaction peak current varies linearly with the square root of scan rate $(v)^{1/2}$, indicative of electrode reaction kinetics controlled by mass transport (semi-infinite linear diffusion) of the reactant. Apparent heterogeneous electron-transfer rate constants, $K°_{app}$, for all seven redox systems have been determined from ΔE_p-v experimental data, according to the method described by Nicholson. $K°_{app}$ values of 1.02-1.17 cm/s have been observed for $Ru(NH_3)_6^{3+/2+}$, $Ir(Cl)_6^{2-/3-}$, and $Fe(CN)_6^{3-/4-}$ without any extensive electrode pretreatment (e.g., polishing). Lower $K°_{app}$ values of 10^{-6}-10^{-2} cm/s have been found for catechol, dopamine, ferrocene monocarboxylic acid, and caffeic acid. The voltammetric responses for $Ru(NH_3)_6^{3+/2+}$, $Ir(Cl)_6^{2-/3}$, and $Fe(CN)_6^{3-/4-}$ have also been examined at SWCNT-modified W electrodes in different solutions *p*H (1.1 –10.0), and the corresponding ΔE_p, i_p^{ox}; i_p^{red}; and $K°_{app}$ values for the most part, have been unaffected by the solution *p*H. This is probably related to the absence of oxygen-functionalities at SWCNT-modified W microelectrodes, which is in contrast to the typical behavior of the oxygenated, sp^2 carbon electrodes, such as glassy carbon or graphite.

IPC Code: Int. Cl.[7] B82B; C25B; H01M4/00; G01N27/00

Carbon nanotubes (CNTs) have become an important subject of research activities since their initial discovery by Iijima[1] in 1991. Several practical applications have been reported as tips in scanning probe microscopy[2-5], as field-effect transistors[6,7], as electronic rectifiers[8], as electrodes for supercapacitors[9,10] and sensors[11-14]. In particular, Single-Walled Carbon Nanotubes (SWCNTs), which can be regarded as quantum wires[15], have raised wide interest for electrochemical applications. So far, some studies have been reported on the electrochemistry of SWCNTs[10,14,16-20]. Luo *et al.*[14] cast the film of SWCNT functionalized with carboxylic acid group on a GC electrode. The SWCNT film modified electrodes show stable cyclic voltammetric behavior and have an efficient catalytic behavior to the biomolecules such as dopamine, epinephrine, and ascorbic acid. Wang *et al.*[18] reported the direct electrochemistry of cytochrome *c* solution at an activated SWCNT film modified electrode. Azamian *et al.*[19] analyzed the interaction between SWCNTs and a variety of metalloproteins and enzymes by AFM. They observed that the enzyme could be immobilized on the tubes with the retention of activity. Guiseppi-Elie *et al.*[20] demonstrated that the flavin adenine dinucleotide (FAD) and glucose oxidase can be adsorbed on unannealed SWCNT and display good electrochemical response.

In our previous work, we investigated the electrochemical performances of SWCNTs-W modified microelectrodes[21] showing interesting results compared with those obtained at GC conventional bare electrodes. In particular, the new nanostructured microelectrodes were applied successfully for the determination of monomamine neurotransmitters as dopamine, epinephrine, and

norepinephrine, which play very important diagnostic roles, are critical for normal neural metabolism, and are involved in some neurological disorders such as Parkinson's disease.

In this paper, we focus on the electrochemical investigations of some probes (i.e. $Fe(CN)_6^{3-/4-}$, $Ru(NH_3)_6^{3+/2+}$, $Ir(Cl)_6^{2-/3-}$, catechol, dopamine, ferrocene monocarboxylic acid and caffeic acid) at different types of nanostructured-modified microelectrodes, to evaluate and to compare the difference in terms of electroanalytical response and apparent heterogeneous electron-transfer rate constants, K°_{app}. For these nanostructured modified-microelectrodes, very interesting results were achieved compared to those obtained at GC conventional bare electrodes, revealing that through the SWCNT platforms the charge transport between the electroactive substrate in solution towards the electrode surfaces, was greatly catalyzed. This phenomenon could be probably related to the very well oriented and aligned nanotube coatings, which act as conductive layer between the redox-active substrates and the electrode transducer surfaces. The effects of morphology and microstructure of the SWCNTs obtained by CVD deposition method at W microwires on controlling the electrical-communication properties (K°_{app}) between the redox probes and the electrode transducers, is also examined and discussed.

Materials and Methods

Electrochemical measurements at SWCNT-modified W microelectrodes

A precise and detailed description is available about the fabrication of SWCNT-modified W microelectrodes using CVD method to deposit SWCNT coatings[21]. Cyclic voltammetry (CV) experiments were performed using an Amel (model 433) polarographic analyzer (Milan, Italy). The electrochemical cell was assembled as a conventional three-electrode system: a working electrode made of W, 300-μm in diameter coated by SWCNT layer, an Ag|AgCl reference electrode (model 805/CPG/6 from Amel, Milan, Italy), and a Pt counter electrode. All experiments were carried out at room temperature. Initial cyclic voltammetry experiments were carried out over the range 5-1000 mV/s, while a scan rate of 100 mV/s was eventually chosen to survey the behavior of the various electrodes being evaluated. All the solutions for the experiments were deoxygenated with N_2 for at least 10 min before each measurement.

Heterogeneous electron-transfer rate constant determination and SWCNTs coating characterization

The apparent heterogeneous electron-transfer rate constant, K°_{app}, for $Fe(CN)_6^{3-/4-}$, $Ru(NH_3)_6^{3+/2+}$, $Ir(Cl)_6^{2-/3-}$, catechol, dopamine, ferrocene monocarboxylic acid and caffeic acid, was determined by cyclic voltammetry (ΔE_p scan rate dependence) following the method developed by Nicholson[22]. ΔE_p varied over the scan rate range tested, with K°_{app} being statistically determined from data at several scan rates.

Morphology of the deposits was studied using a Hitachi S-4000 Field-Emission Scanning Electron Microscopy (FEG-SEM). The structural characteristics of the various materials were analyzed by Raman spectroscopy. The Raman spectra were collected at room temperature in the backscattering configuration using a Ar-ion laser beam (λ: 514.5 nm; spectral resolution: 3 cm^{-1}).

Potassium ferricyanide, hexaammineruthenium(III) chloride, sodium hexachloroiridate(III) hydrate, catechol, dopamine, ferrocene monocarboxylic acid, and caffeic acid were obtained from Sigma (St. Louis, MO). All the chemicals from commercial source were of analytical grade. The solutions were prepared using 0.1*M* phosphate buffer (*p*H 7.0). Standard solutions were prepared daily in the same buffer. For the studies on the effect of *p*H, solutions of 0.1*M* phosphate buffer with 5m*M* potassium ferricyanide, 5m*M* hexaammineruthenium(III) chloride, and 5m*M* hexachloroiridate(III) hydrate; at *p*H values of 1.90, 7.00, and 10.00 were prepared using the appropriate molar ratios of phosphoric acid, sodium phosphate dibasic, and sodium phosphate. The insulating varnish was purchased from RS (Milan, Italy).

Results and Discussion

Voltammetric characteristics and kinetic performances at SWCNT-modified W microelectrodes

In Fig. 1 are reported the FEG-SEM pictures of SWCNT deposits on W microwires, as obtained by CVD method, widely described in ref. (21). Background voltammetric $I(\mu A)/cm^2$-E curves can be very informative about the SWCNT films quality (i.e. presence of functional chemical groups at the electrode surface) and electrical conductivity. Figure 2 shows cyclic voltammetric $I(\mu A)/cm^2$-E curves for SWCNT-modified W microwire electrodes in 0.1 *M* phosphate buffer solution, *p*H 7.00. The response for glassy carbon (different geometric areas — for GC bare disk planar electrode is 0.031 ± 0.003 cm^2,

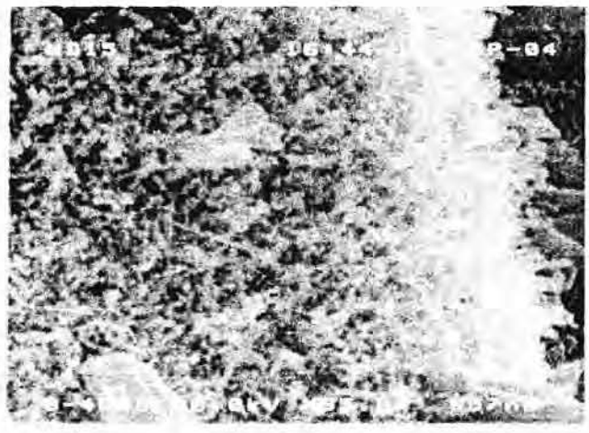

Fig. 1—FEG-SEM image of SWCNT coating deposited on tungsten/W microelectrodes.

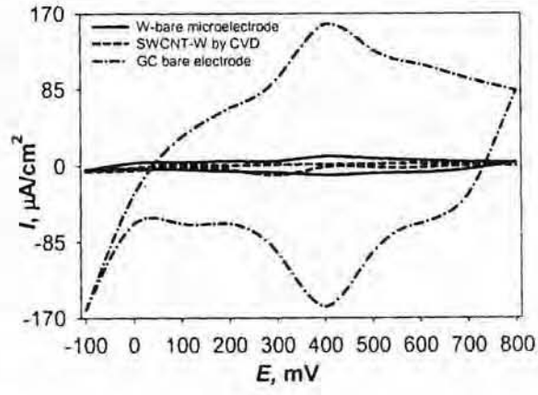

Fig. 2—Cyclic voltammograms of current density I (μA)/cm^2-E curves for the SWCNT-modified microelectrode types in 0.1 *M* phosphate buffer, *p*H 7.0. [Scan rate: 100 mV/s; geometric area of cylinder microelectrodes: 0.047 cm^2; with tip diameter of microwires: 300 micron; for GC bare conventional electrode, the geometric area is: 0.031 cm^2; with the disk diameter of 2 mm].

whereas for W cylindrical wires, it is 0.047± 0.003 cm^2) is also presented for comparison. The curves for the W wires are, for the most part, featureless with the same current magnitude, which is a factor of ≈ 10 less than glassy carbon. The response for glassy carbon shows a redox couple centered at ≈ 300 mV, which is associated with redox-active surface carbon-oxygen functional groups terminating the edge plane and defect sites[26]. SWCNT grown directly on W-microelectrode surfaces (tip) did not present functional groups (carbon-oxygen groups), as expected, and therefore, redox peaks are often not evident in the voltammograms. The lower background current density I(μA)/cm^2 for the SWCNT-modified W microelectrodes leads to improved signal-to background ratios and results in: (i) a reduced pseudocapacitance, because of the absence of the redox-active or ionizable surface functional groups, and (ii) in a reduced capacitance, due to a slightly lower internal charge carrier concentration.

Cyclic voltammetry was used to study the electrode response for $Fe(CN)_6^{3-/4-}$, $Ru(NH_3)_6^{3+/2+}$, $Ir(Cl_6)^{2-/3-}$, catechol, dopamine, ferrocene monocarboxylic acid and caffeic acid. Cyclic voltammetric i-E curves for all seven redox systems, at a scan rate of 100 mV/s, are presented in Figs 3, and 4, and at SWCNT-modified W microelectrodes fabricated by CVD deposition method. A summary of the cyclic voltammetric data for the investigated SWCNT-modified W microelectrodes, and GC bare electrode for comparison, is presented in Table 1, where ΔE_p and I_{pa} /I_{pc} values are presented for a single scan rate (100 mV/s).

The absence of relevant background current density I(μA)/cm^2 (Fig. 2) provided flexibility in the choice of scan rate so as to optimize analytical performance and signal/noise ratio and 100 mV/s was then chosen in consideration of the scan rates known to be advantageous for the biological analytes of interest (dopamine, catechol, ferrocene monocarboxylic acid, and caffeic acid). For kinetic investigations scan rate range of 5-500 mV/s was used but for biological molecules (i.e. dopamine, catechol, ferrocene monocarboxylic acid, and caffeic acid) the range 50-500 mV/s was used for the advantage described above.

It is evident that the electrochemical responses are reversible for all the substrates investigated at SWCNT-W microelectrodes (see Figs 3 and 4) with lower ΔE_p (mV) values (in order to reduce the interference effects) and higher I (μA) values, compared to those reported at Glassy Carbon conventional bare electrodes (see Table 1). High current values recorded at SWCNT-modified W microelectrodes could be related to the high electrical conductivity of carbon nanotubes coating, and also to the particular geometry of the W microelectrode (cylindrical geometry of SWCNT-modified W microelectrodes)[21]. In addition, the electrochemical area estimated by chronocoulometry[21] demonstrated the largest surface area available at carbon nanostructured materials firstly responsible for the higher current values observed. The electrode responses, in terms of ΔE_p (mV) and I_{pa}/I_{pc} (μA) were

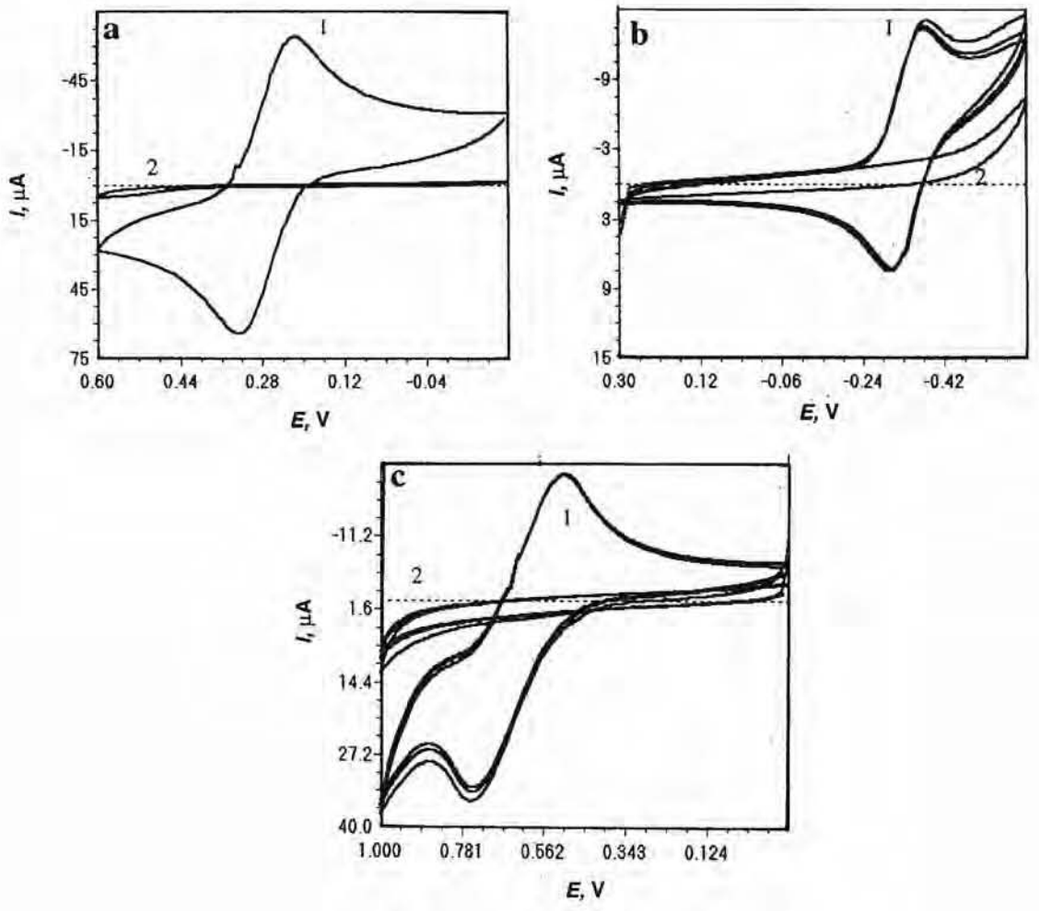

Fig. 3—Cyclic voltammograms at SWCNT-modified W microelectrode for (a) 5m*M* potassium ferricyanide; (b) 5 m*M* hexaammineruthenium(III) chloride; (c) 5 m*M* sodium hexachloroiridate(III) hydrate. [Experimental conditions: 0.1 *M* phosphate buffer solution, *p*H = 7.0; scan rate: 100 mV/s (curve 1). Curve 2: electrochemical superimposed responses of the same solutions at bare W; and W/carbide microelectrodes; and in 0.1 *M* phosphate buffer solution ($i_{background}$) at bare W; and W/carbide; and SWCNT-W modified microelectrodes. SWCNT-modified W microelectrode: tip diameter: 300 μm; length: 0.5 cm].

very reproducible over 250th continuous cycles for $Fe(CN)_6^{3-/4-}$, $Ru(NH_3)_6^{3+/2+}$, $Ir(Cl_6)^{2-/3-}$, (Fig. 5), and after 250th cycle, the electrochemical signal decreased only for 30% of the original one (1st cycle). A very important result concerns the operational stability observed also for dopamine, catechol, ferrocene monocarboxylic acid, and caffeic acid, for 250th continuous cycles. After the 250th cycle, the electroanalytical signal for these biological molecules, decreased only for 50 % of the original ones. Dopamine and other important monoamines are widely known to produce adsorption phenomena at conventional bare graphite electrodes[38,39], promoted by the introduction of sp^2 carbon impurities, and many oxygen-functional groups (e.g., carboxylic acid, carbonyl type, alchols, etc.)[23-26]. The great advantages to use SWCNT-W modified microelectrodes in order to minimize adsorption phenomena of biological probes at the electrode surfaces[27, 28], come from: (i) the higher surface area, typical of SWCNTs (SWCNTs surface area[40,41] of: 300 m^2/g; graphite surface area of: 20 m^2/g), which have a larger density of redox-active centers, and (ii) the absence of oxygen-functional groups[28] at SWCNT layer, deposited by CVD directly on W microwires, as described in our previous work[21].

The reproducibility for our SWCNT-modified W microelectrodes is routinely better that 1% for the SWCNT-modified W microelectrodes fabricated during the same CVD deposition step (intra-reproducibility); and 3% for modified microelectrodes obtained during different CVD deposition step (inter-

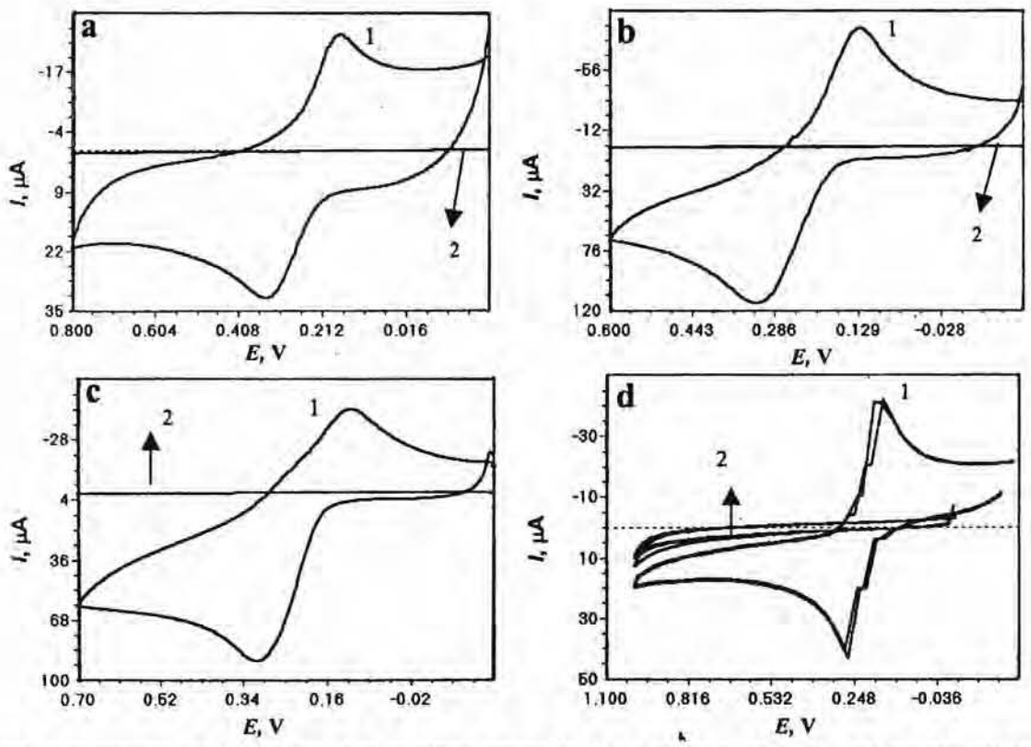

Fig. 4—Cyclic voltammograms at SWCNT-modified W microelectrode for (a) 0.1 m*M* dopamine; (b) 1 m*M* catechol; (c) 1m*M* caffeic acid; and (d) 1 m*M* ferrocene monocarboxylic acid. [Experimental conditions: 0.1 *M* phosphate buffer solution, *p*H = 7.0; scan rate: 100 mV/s (curve 1). Curve 2: electrochemical superimposed responses of the same solutions at bare W; W/carbide microelectrodes; and in 0.1 *M* phosphate buffer solution ($i_{background}$) at SWCNT-W; W/carbide, and W bare microelectrodes. SWCNT-modified W microelectrode: tip diameter: 300 μm; length: 0.5 cm].

Table 1— Summary of the cyclic voltammetric data for several redox systems at SWCNT-modified W electrode by CVD method. [tip diameter 300 μm; length, 0.5 cm; and at GC bare electrode (2 mm diameter)]

Molecules	[a]E_{pa}(mV)		[a]E_{pc}(mV)		[a]ΔE_p(mV)		[b]I_{pa}(μA)/cm^2		[b]I_{pc}(μA)/cm^2		I_{pa}/I_{pc}	
$Fe(CN)_6^{3-/4-}$ 5 mM	1	2	1	2	1	2	1	2	1	2	1	2
	310.0	320.0	250.0	260.0	60.0	60.0	1383.0	290.3	-1329.8	-274.2	1.0	1.1
$Ru(NH_3)_6^{3+/2+}$ 5 m*M*	-300.0	-310.0	-380.0	-398.0	80.0	88.0	276.6	258.1	-276.6	-209.7	1.0	1.2
$Ir(Cl)_6^{2-/3-}$ 5 m*M*	700.0	710.0	-542.0	-543.2	158.0	166.8	744.7	371.0	-712.8	-338.7	1.0	1.1
Ferrocene Mc acid, 1 m*M*	410.0	400.0	320.0	300.0	90.0	100.0	340.4	338.7	-331.9	-293.5	1.0	1.1
Catechol 1 m*M*	260.0	250.0	160.0	150.0	100.0	100.0	2425.5	2267.7	-1957.4	-1935.5	1.1	1.2
Dopamine 0.1 m*M*	300.0	300.0	210.0	200.0	90.0	100.0	553.2	483.9	-531.9	-458.1	1.0	1.1
Caffeic acid 1 m*M*	300.0	335.0	160.0	170.0	140.0	165.0	1489.4	774.2	-1446.8	-638.7	1.0	1.2

1: SWCNT- modified W microelectrodes; 2: Conventional GC bare electrode.

[a]ΔE_p (mV) for all the reversible electrochemical species as: potassium ferricyanide, catechol, hexaammineruthenium(III) chloride, sodium hexachloroiridate(III) hydrate, ferrocene monocarboxylic acid, dopamine, caffeic acid. Cyclic voltammograms were carried out in 0.1 *M* phosphate buffer solution, *p*H 7.0 at scan rate of 100 mV/s.

[b] I_{pa} (μA)/cm^2 is the current density value of the anodic peak and I_{pc} (μA)/cm^2 is the current density value of the cathodic peak for all the electroactive reversible species investigated.

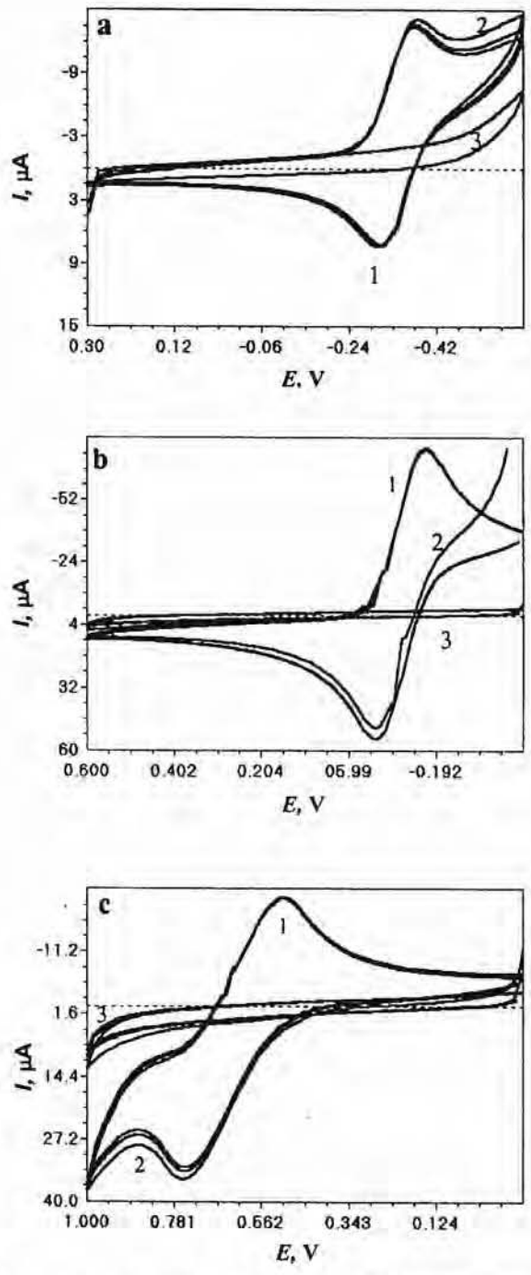

Fig. 5—Cyclic voltammograms at SWCNT-modified W microelectrodes for (a) 5 m*M* hexaammineruthenium(III) chloride; (b) 5 m*M* potassium ferricyanide; and (c) sodium hexachloroiridate(III) hydrate, in 0.1 *M* phosphate buffer solution, *p*H =7, (curve 1); the same at the 250th cycles from microelectrode assembling, working at the same electrode surfaces (curve 2), and the electrochemical responses in 0.1 *M* phosphate buffer solution, *p*H 7.0 (curve 3, $i_{background}$). [Scan rate: 100 mV/s; potential window: -0.2 - +0.6 V vs. Ag/AgCl reference electrode. SWCNT-modified W microelectrode: tip diameter: 300 mm; length: 0.5 cm].

reproducibility). The reproducibility was also an important aspect to consider here because variable pre-treatment procedures can affect the electrode /surface microstructure and chemistry differently. Therefore, for the redox systems, pre-treatments can lead to significant response variability and a very low reproducibility of the analytical signal[29]. In this work, the forward reaction peak currents varied linearly with the square root of scan rate, $(\nu)^{1/2}$, for potassium ferricyanide, indicating that the electrode kinetics are controlled by mass transport (semi-infinite linear diffusion) of the reactant (see Fig. 6a, where scan rates range from 5-1000 mV/s). Similarly, diffusion-controlled electron transfer at these SWCNT-modified W microelectrodes was also found for ferrocene monocarboxylic acid (Fig. 6b) confirming that for biological system also no-adsorption phenomena were detected at SWCNT-modified W microelectrodes.

For kinetic evaluations, K°_{app} was calculated from the variation of ΔE_p with scan rate, ranging from 5-500 mV/s for $Fe(CN)_6^{3-/4-}$; $Ru(NH_3)_6^{3+/2+}$; $Ir(Cl_6)^{2-/3-}$, and 50-500 mV/s for dopamine, catechol, ferrocene monocarboxylic acid and caffeic acid. K°_{app} values are listed in Table 2 along with the range of scan rates over which they were determined. In this work, we refer to the rate constant as apparent, because no correction for any electric double layer effects was made. Finally, some comparison rate constant data for glassy carbon are given, too (Table 2). For all the seven electroactive probes low ΔE_p values are seen for a wide scan rate range, and the I_{pa}/I_{pc} peak current ratio is near 1, meaning that the electron-transfer reactions were easily catalyzed on the carbon nanotube-modified microelectrode surfaces (ΔE_p were near to Nernst's value demonstrating reversibility for all the probes investigated). Standard deviations in K°_{app} of about 1% are seen, and importantly, the deviation does not depend on the scan rate. This indicates that the ΔE_p values, hence the K°_{app} values, are not significantly affected by uncompensated ohmic resistance (both the solution and electrode) within the cell. K°_{app} for $Ru(NH_3)_6^{3+/2+}$ and $Ir(Cl)_6^{2-/3-}$ is one order of magnitude higher than that reported for pre-treated and freshly activated glassy carbon[30,31], and their values ranging from 1.078 – 1.140 cm/s (Table 2). This result is probably related to the larger surface area of SWCNT materials and also to their physical and chemical properties[32,33], as electrical conductivity, and their length. In fact, it seems that the SWCNT acts as a conductive layer between the

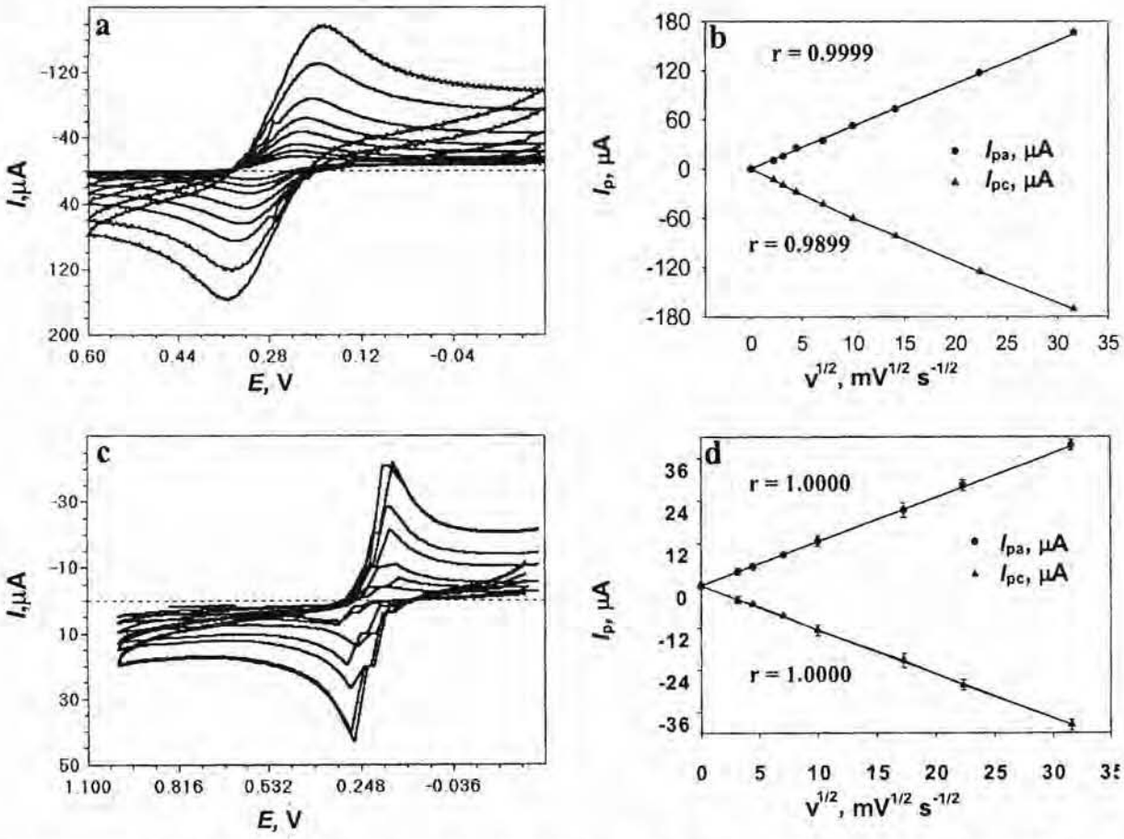

Fig. 6— (a): Cyclic voltammetry of 1m*M* potassium ferricyanide in 0.1 *M* phosphate buffer solution (*p*H 7.0) on SWCNT-coated W microelectrodes at scan rates: 5, 10, 20, 50, 100, 200, 500, 1000 mV/s; (b): The corresponding plot of the catalytic current against the square root of different scan rates; 5-1000 mV/s; (c) Cyclic voltammetry of 1m*M* ferrocene monocarboxylic acid in 0.1 *M* phosphate buffer solution (*p*H 7.0) on SWCNT-coated W microelectrodes at scan rates: 5, 10, 20, 50, 100, 200, 500, 1000 mV/s; (d): The corresponding plot of the catalytic current against the square root of different scan rates; 5-1000 mV/s, for 1m*M* ferrocene monocarboxylic acid.

redox-active substrates and the electrode transducer surfaces, as reported in refs 34-36. So the electrons are transported along distances greater than 150 nm and the rate of electron transport is controlled by the length of the SWCNTs, and its results significantly improved at the nanostructured-modified electrodes, where the diameter/length ratio is very low (all SWCNT's physical-chemical properties are because of this).

$K°_{app}$ for $Fe(CN)_6^{3-/4-}$ shows values one order of magnitude higher compared to those observed at GC bare electrodes, ranging from 1.037-1.058 cm/s, but lower than those obtained for $Ru(NH_3)_6^{3+/2+}$and $Ir(Cl)_6^{2-/3-}$. This effect is probably related to the particular redox-system, $Fe(CN)_6^{3-/4-}$, which is of the inner-sphere type[37-40], with the electrode kinetics being highly sensitive to the electrode material surface terminations[37-40], like carbonyl functional groups. For SWCNT-W modified microelectrodes used here, no oxygen functionalities were present at the electrode surfaces[21], and this is presumably the reason why $K°_{app}$ for $Fe(CN)_6^{3-/4-}$ is lower as compared to that of $Ru(NH_3)_6^{3+/2+}$ and $Ir(Cl)_6^{2-/3-}$. In fact, the last redox systems, $Ru(NH_3)_6^{3+/2+}$ and $Ir(Cl)_6^{2-/3-}$, proceed by an outer-sphere electron-transfer pathway with the electrode kinetics being relatively insensitive to the surface carbon-oxygen functionalities[36,37], specifically carbonyl functional groups. For all the other electroactive probes, as dopamine, catechol, ferrocene monocarboxylic acid and caffeic acid, $K°_{app}$ values (Table 2) resulted in one order of magnitude higher than that calculated at GC bare electrodes, but lower if compared to those calculated for $Fe(CN)_6^{3-/4-}$, $Ru(NH_3)_6^{3+/2+}$ and $Ir(Cl)_6^{2-/3-}$ (Table 2). DuVall and McCreery[41-44] demonstrated that removing surface impurities and putting oxygen

Table 2—Cyclic voltammetric and heterogeneous electron-transfer rate constant data for seven redox systems at SWCNT- modified W microelectrodes[a] by CVD method. [W tip diameter 300 μm; length, 0.5 cm]

Analytes	Scan rate	ΔE_p	I_p^{ox} / I_p^{red}	K^o_{app}	K^{o}_{app} [b] For Glassy Carbon (GC)[b]
	(mV/s)	(mV)		(cm/s)	(cm/s)
	5	60.0	1.00	1.056	
$Fe(CN)_6^{3-}$	10	58.0	1.00	1.058	0.100 ± 0.020
$\alpha = 0.50$	20	59.0	1.01	1.057	
	50	60.0	1.00	1.056	
	100	60.0	1.01	1.056	
	500	95.0	1.01	1.037	
	5	158.0	1.00	1.120	
$IrCl_6^{2-}$	10	154.0	1.00	1.140	0.500 ± 0.060
$\alpha = 0.50$	20	156.0	0.98	1.130	
	50	160.0	0.97	1.104	
	100	158.0	1.00	1.120	
	500	172.0	1.09	1.083	
	5	80.0	1.00	1.094	
$Ru(NH_3)_6^{3+}$	10	75.0	0.98	1.110	0.240 ± 0.070
$\alpha = 0.50$	20	80.0	0.98	1.094	
	50	78.0	1.01	1.098	
	100	80.0	1.10	1.094	
	500	98.0	1.08	1.078	
	5	86.0	1.00	5.500×10^{-7}	
Ferrocene	10	89.0	1.00	5.310×10^{-7}	$(6.560 \pm 0.340) \times 10^{-8}$
monocarboxylic acid	20	88.0	1.08	5.324×10^{-7}	
$\alpha = 0.68$	50	89.0	1.00	5.310×10^{-7}	
	100	90.0	1.09	5.250×10^{-7}	
	500	110.0	1.20	5.203×10^{-7}	
	50	80.0	1.00	3.360×10^{-2}	
Dopamine	100	86.0	1.10	3.300×10^{-2}	$(3.340 \pm 0.250) \times 10^{-3}$
$\alpha = 0.88$	500	100.0	1.20	3.230×10^{-2}	
	50	90.0	1.00	6.454×10^{-7}	
Caffeic acid	100	120.0	1.00	6.120×10^{-7}	$(6.786 \pm 0.285) \times 10^{-8}$
$\alpha = 0.65$	500	130.0	1.10	5.452×10^{-7}	
	50	90.0	1.00	9.120×10^{-6}	
Catechol	100	100.0	1.10	8.500×10^{-6}	$(5.510 \pm 0.302) \times 10^{-7}$
$\alpha = 0.45$	500	120.0	1.20	7.300×10^{-6}	

[a]The supporting electrolyte for all the reversible probes was 0.1 *M* phosphate buffer solution, *p*H 7.00. Heterogeneous electron-transfer rate constants for all the substrates, as well as all the corresponding α values, were determined from ΔE_p-ν trends , as described in reference (49); and references cited therein. [b] GC bare electrode heterogeneous electron-transfer rate constants from references [30,31 and references cited therein].

functional groups (as carboxylic acid, and carbonyl functional groups) to increase adsorption sites on glassy carbon resulted in an increase in the electron-transfer rate for catechols[45]. Their work demonstrates the vital role adsorption plays in the electron-transfer process, effects that may involve changes in the reorganization energy. In fact, there is a large energy barrier for reorganizing the solvation sphere around the redox center following electron transfer. The carbonyl functional groups serve to lower this energy barrier, apparently by forming a bridging complex with the reactant at the electrode surface[46].

Anything that inhibits the adsorption (e.g., surface/electrode modification) of catechols and other biological molecules, also inhibits the electrode kinetics. In other works[47-50], the adsorption of dopamine can be promoted by the introduction of sp^2 carbon impurities and many oxygen-functional groups (e.g, carboxylic acid, carbonyl groups, alcohols, etc.)[47-50]. Considering these effects, the absence of functional groups at the SWCNT-modified W microelectrodes could be able to explain the lower K°_{app} values, ranging from $7.0 \times 10^{-6} - 3.0 \times 10^{-2}$ cm/s for biological substrates, like dopamine, catechol, ferrocene monocarboxylic acid, and caffeic acid.

At the same time, the higher values of K°_{app} obtained for these biological substrates at SWCNT-modified W microelectrodes (compared to those obtained at GC bare electrodes, Table 2) could be explained invoking the physical and chemical properties of the nanostructured coating, which resulted in very well oriented and perpendicularly aligned at the W microwire-modified electrodes (as shown in Fig. 1); with a larger surface area[21], and finally, a particular W-microelectrode cylindrical geometry, responsible for high diffusion current values recorded at SWCNT-modified W microelectrodes.

Further investigations will be carried out to verify and study the K°_{app} dependences for these electrochemical probes, from many factors such as the surface chemistry of nanostructures; the last used to assemble electrode transducers. It is reasonable to suppose that the next step of this work will concern the assembling of microelectrodes using chemically treated Single-Wall Carbon Nanotubes having oxygen-chemical groups, in order to enlighten the role of the carbonyl groups during the electron transfer reactions at the electrode surfaces.

The *p*H effects on voltammetric response at SWCNT-modified W microelectrodes

The response for charged redox analytes at non-functionalized SWCNT-modified W microelectrodes should be unaffected by solution *p*H because of the absence of ionizable surface oxides[21]. To test this hypothesis, the cyclic voltammetric responses for $Fe(CN)_6^{3-/4-}$, $Ir(Cl_6)^{2-/3-}$, and $Ru(NH_3)_6^{3+/2+}$ were examined at *p*H 1.90, 7.00, and 10.00—below and above the expected pK_a of the carboxylic acid functional groups. Table 3 presents a summary of the results for all the electrical charged probes investigated. Generally speaking, there is a minimal effect of solution *p*H on the ΔE_p and K°_{app} values for these investigated three redox systems. K°_{app} standard deviation is lower than 1% at three different *p*H values, for all three redox charged systems, at SWCNT-modified W microelectrodes. This result is consistent with low-oxide, non-functionalized electrode surfaces.

These carbonyl, and carboxylic acid functional groups generally terminate the "edge" plane and defects sites of the electrode materials. They form naturally, during exposure to the atmosphere (air/H_2O), and are introduced during pre-treatment (e. g. mechanical polishing; anodic/cathodic polarization; chemical oxidation, or physical treatments). These oxygen-functionalities influence the chemical and electrochemical properties of the carbon electrode surface, playing key roles in the electric double layer structure and the extent of analyte adsorption. Carboxylic acid functional groups are common on oxygen-containing glassy carbon surfaces, and conventional graphite[51-55]. The pK_a of such surface functionalities appears[55] to be near 4.5. Therefore, depending on the solution *p*H, these groups can either be protonated (uncharged) or deprotonated (negatively charged). Highly charged redox systems can be affected by the presence of these ionizable functional groups (e.g. excess surface charge). For example, ΔE_p for anionic redox system, such as $Fe(CN)_6^{3-/4-}$ or $Ir(Cl)_6^{2-/3-}$ becomes strongly *p*H dependent, increasing significantly when these functional groups are deprotonated. On the other hand, ΔE_p for a cationic redox system, such as $Ru(NH_3)_6^{3+/2+}$, is reduced when these functional groups are deprotonated. For instance, Deakin *et al.* observed that K°_{app} for $Fe(CN)_6^{3-/4-}$ or $Ir(Cl)_6^{2-/3-}$ decreases with increase in *p*H from 2 to 8, while K°_{app} for $Ru(NH_3)_6^{3+/2+}$ increases[56]. The larger ΔE_p for

Table 3—Cyclic voltammetric and heterogeneous electron-transfer rate constant data for three redox-charged systems at SWCNT-modified W microelectrodes by CVD, as a function of the solution *p*H[a]. [W tip diameter 300 μm; length, 0.5 cm]

Analytes	Scan rate (mV/s)	ΔE_p (mV)		K°_{app} (cm/s)	
		*p*H	*p*H	*p*H	*p*H
		1.90	10.00	1.90	10.00
	5	58.0	69.0	1.066±0.004	1.048±0.01
$Fe(CN)_6^{3-}$	10	55.0	68.9	1.072±0.002	1.050±0.02
α= 0.50	20	56.0	70.0	1.070±0.001	1.040±0.004
	50	58.5	70.0	1.064±0.004	1.040±0.002
	100	55.0	69.9	1.072±0.002	1.042±0.01
	500	56.0	72.0	1.070±0.001	1.036±0.02
	5	147.0	168.0	1.220±0.01	1.101±0.0008
$IrCl_6^{2-}$	10	147.0	168.0	1.220±0.0007	1.101±0.01
α= 0.50	20	145.0	170.0	1.253±0.02	1.085±0.004
	50	146.0	169.0	1.212±0.01	1.090±0.002
	100	147.0	168.0	1.220±0.003	1.101±0.01
	500	145.0	169.0	1.253±0.004	1.090±0.02
	5	88.0	70.0	1.100±0.01	1.134±0.004
$Ru(NH_3)_6^{3+}$	10	90.0	75.0	1.090±0.004	1.125±0.002
α= 0.50	20	90.0	76.0	1.090±0.02	1.120±0.01
	50	94.0	70.0	1.080±0.002	1.134±0.02
	100	89.0	74.0	1.094±0.0007	1.128±0.003
	500	90.0	75.0	1.090±0.004	1.125±0.01

[a] The supporting electrolyte for three redox-charged systems was 0.1 *M* phosphate buffer solution, at *p*H 1.90, and 10.00. Heterogeneous electron-transfer rate constants, as well as the corresponding α values, were determined from ΔE_p-ν trends.

$Fe(CN)_6^{3-/4-}$ and smaller value for $Ru(NH_3)_6^{3+/2+}$, when there is excess negative surface charge, reflects more sluggish and more rapid electrode kinetics, respectively, because of electrostatic repulsion and attraction (e.g. electric double layer effects). Electrostatic repulsion of $Fe(CN)_6^{3-/4-}$ leads to a greater electron tunneling distance and more sluggish electrode kinetics. The opposite trend holds true for $Ru(NH_3)_6^{3+/2+}$.

Considering all these aspects, further work is required for assembling W-microelectrodes with functionalized SWCNT material in order to study the relationship between kinetics (i.e, K°_{app}) and the surface chemistry (i.e. carbonyl and carboxylic acid functional groups) at SWCNT-modified W microelectrodes, which plays a key role during the electron-transfer processes.

Conclusions

The electrochemical performances at SWCNT-modified W microelectrodes, and also the apparent heterogeneous electron-transfer rate constants, K°_{app} were compared with those of GC bare electrodes. Better results in terms of stability, reproducibility and electrode kinetics (K°_{app} values) were obtained at SWCNT-modified W microelectrodes fabricated by CVD method. All these electrodes exhibited a low and stable background current, a factor of ≈10 lower than a bare/conventional glassy carbon electrode. Apparent heterogeneous electron-transfer rate constants, K°_{app} for $Fe(CN)_6^{3-/4-}$, $Ru(NH_3)_6^{3+/2+}$, $Ir(Cl)_6^{2-/3-}$, were in the mid 1.037 to low 1.140 cm/s range, without extensive electrode pre-treatment, and these results are one order of magnitude higher than those calculated at GC bare electrodes. K°_{app} for dopamine, catechol, ferrocene monocarboxylic acid, and caffeic acid, was much lower if compared to those calculated for the inorganic probes (see above) ranging from $7.0 \times 10^{-6} - 3.0 \times 10^{-2}$ cm/s. These last resulted in higher than the corresponding values obtained at GC bare electrodes. The improved kinetic performances observed at SWCNT-modified W

microelectrodes could be related to the excellent properties of Single-Wall Carbon Nanotubes; i.e. high surface area, high electrical conductivity, this last properly related to nanostructured physical and chemical properties, and also a particular geometry for SWCNT-modified W microelectrodes. The lower values of K°_{app} obtained for biological molecules, could be probably related to the absence of oxygen-functional groups at SWCNT-modified W electrode surfaces. The lack of adsorption, probably related to the absence of ionizable carbon-oxygen functionalities anchored at SWCNT-modified W electrode surfaces, could explain also the absence of *p*H effects. In fact, for $Fe(CN)_6^{3-/4-}$, $Ru(NH_3)_6^{3+/2+}$ and $Ir(Cl)_6^{2-/3-}$, K°_{app} was relatively independent of the solution *p*H because of surface carbon-oxygen functionalities, particularly, those that are ionizable (e.g. carboxylic acid, $pK_a \approx 4.5$), can strongly influence the carbon electrode response (as routinely observed for glassy carbon and graphite, as the surface normally contains carbon-oxygen functionalities).

In conclusion, it is evident that the improved electron-transfer mechanisms, and therefore the kinetic performances observed at Single-Walled Carbon Nanotubes-modified W microelectrodes, combined with their reproducibility and stability for several electroactive substrates, could enhance the interest of the scientific world towards new nanostructured-modified devices for future biological, medical, and electronic applications.

Acknowledgement

This work was generously supported by the Department of Chemistry in Tor Vergata University, Rome (Italy), and the ISMN CNR Division II, Rome (Italy). The technical assistance of ISMN Institute and laboratories is greatly appreciated, as always.

References

1 Iijima S & Ichihashi T, *Nature*, 363(1993) 603.
2 Willner I, *Science*, 298(2002)2407.
3 Ajayan P M & Iijima S, *Nature*, 361(1993)333.
4 Hamada N, Sawada S & Oshiyama A, *Phys Rev Lett*, 68 (1992)1579.
5 Aihara J, Yamabe T & Hosoya H, *Synth Met*, 64(2-3) (1994)309.
6 Saito R, Dresselhaus G & Dresselhaus M S, *Physical Properties of Carbon Nanotubes* (Imperial College Press, London) 1998.
7 Rao C N R, Satishkumar B C, Govindaraj A & Nath M, *Chem Phys Chem*, 2(2001)78.
8 Baughman R H, Cui C, Zakhidov A A, Iqbal Z, Barisci J N, Spinks G M, Wallace G G, Mazzoldi A, De Rossi D, Rinzler A G, Jaschinski O, Roth S & Kertesz M, *Science*, 284(1999)1340.
9 Tans S J, Verschueren R M & Dekker C, *Nature*, 393 (1998)49.
10 Derycke V, Martel R, Appenzeller J & Avouris P, *Nano Lett*, 1(2001) 453.
11 Yu X, Chattopadhyay D, Galeska I, Papadimitrakopoulos F & Rusling J F, *Electrochem Commun*, 5(2003)408.
12 Dai L & Mau W H, *Adv Mater*, 13(2001)899.
13 Bachtold A, Hadley P, Nakanishi T & Dekker C, *Science*, 294(2001)1317.
14 Zhao Y-D, Zhang W-D, Chen H & Luo Q M, *Anal Sci*, 18(2002)939.
15 Heller A, *Acc Chem Res*, 23(1990)128.
16 Heller A, *J Phys Chem*, 96 (1992)3579.
17 (a) Willner I & Katz E, *Angew Chem*, 112(2000)1230; (b) Willner I & Katz E, *Angew Chem Int Ed*, 39(2000)1180.
18 Wang J, Li M, Shi Z, Li N & Gu Z, *Anal Chem*, 74(2002)1993.
19 Azamian B R, Davis J J, Coleman K S, Bagshaw C B & Green M L H, *J Am Chem Soc*, 124(2002)12664.
20 Guiseppi-Elie A, Lei C, Baughman R H, *Nanotechnology*,13(5) (2002)559.
21 Valentini F, Orlanducci S, Tamburri E, Terranova M L, Curulli A & Palleschi G, *Electroanalysis*, 17(2005) 28.
22 Nicholson R S, *Anal Chem*, 37(11) (1965)1351.
23 Stotter J, Zak J, Behler Z, Show Y & Swain G M, *Anal Chem*, 74(23) (2002)5924.
24 Martin H B & Morrison P W (Jr), *Electrochem Solid-State Lett*, 4(4) (2001)E17.
25 Haymond S, Zak J K, Show Y, Butler J E, Babcock G T & Swain G M, *Anal Chim Acta*, 500 (2003)137.
26 Krysinski P, Show Y, Stotter J & Blanchard G J, *J Am Chem Soc*, 125(42) (2003)12726.
27 Peigney C H, Laurent E, Baesa Flahaut R R & Rousset A, *Carbon*, 39(2001)507.
28 Firm documentation, Aldrich (U.S.A.).
29 Hu I-F, Karweik D H & Kuwana T, *J Electroanal Chem Interfacial Electrochem*, 188(1-2) (1985)59.
30 Fagan D T, Hu I-F & Kuwana T, *Anal Chem*, 57(1985)2759.
31 Swain G M, in *Electroanalytical Chemistry*, edited by A J Bard and I Rubinstein, (Marcel Dekker, New York) (2003) Vol 22, p. 181.
32 Xiao Y, Patolsky F, Katz E, Hainfeld J F & Willner I, *Science*, 299 (2003)1877.
33 Ajayan P M, *Chem Rev*, 99(1999)1787.
34 Patolsky F, Weizmann Y & Willner I, *Angew Chem Int Ed*,43(2004)2113.
35 Show Y, Witek M A, Sonthalia P & wain G M, *Chem Mater*, 15(2003)879.
36 Williams K A, Veenhuizen P T M, De La Torre B G, Eritjia R & Dekker C, *Nature*, 420 (2002)761.
37 Rao T N, Yagi I, Miwa T, Tryk D A & Fujishima A, *Anal Chem*, 71(13) (1999)2506.
38 Chen Q, Gruen D M, Krauss A R, Corrigan T D, Witek M & Swain G M, *J Electrochem Soc*, 148(1) (2001)E44.
39 Granger M C, Witek M, Xu J, Wang J, Hupert M, Hanks A, Koppang M D, Butler J E, Lucazeau G, Mermoux M, Strojek J W & Swain G M, *Anal Chem*, 72(16) (2000)3793.

40 Swain G M, in *Thin Film Diamond*, edited by C Nebel and J Risten, (Elsevier, Amsterdam), Chap 12 (In press).
41 DuVall S H & McCreery R L, *J Am Chem Soc*, 122(2000) 6759.
42 Granger M C & Swain G M, *J Electrochem Soc*, 146(12) (1999)4551.
43 Bennett J A, Wang J, Show Y & Swain G M, *J Electrochem Soc*, (In press).
44 Deakin M R, Stutts K J & Wightman R M, *J Electroanal Chem Interfacial Electrochem*, 182 (1985)113.
45 Xu J, Granger M C, Chen Q, Lister T E, Strojek J W & Swain G M, *Anal Chem*, 69(19) (1997)591A.
46 Stotter J, Zak J, Behler Z, Show Y & Swain G M, *Anal Chem*,74(23) (2002)5924.
47 Swain M V, James N L, Woodard J C &McCulloc, *Diamond Related Mater*, 12 (2003) 178.
48 Chen P & McCreery R L, *Anal Chem*, 68(1996)3958.
49 Fischer E A, Show Y & Swain G M, *Anal Chem*, 76 (2004) 2553.
50 Wu B, Zhang J, Wei S, Cai S & Liu Z, *J Phys Chem*,105(2001)5075.
51 Chattopadhyay D, Galeska I & Papadimitrakopoulos F, *J Am Chem Soc*, 123(2001)9451.
52 Liu Z, Hou S & Ying L, *Langmuir*, 16(2000)3569.
53 Diao P, Liu Z, Wu B, Wu X, Nan J, Zhang J & Wie Z, *Chem Phys Chem*, 3 (2002)898.
54 Walters D A, Ericson L M, Casavaut M J, Liu J, Colbert D T, Smith K A & Smalley R E, *Appl Phys Lett*, 74(1999)3803.
55 Deakin M R, Kovach P M& Wightman R M, *J Phys Chem*, 90(19) (1986)4612.